

Two-step approach to 3D gravity inversion: case study in the State of Utah

Michael S. Zhdanov, Michael Jorgensen *, and Le Wan, Consortium for Electromagnetic Modeling and Inversion, University of Utah, and TechnoImaging

Summary

We present the methodology and the results of 3D inversion of Bouguer gravity anomaly in the Utah State. The inversion of the regional gravity data can contribute in the development of the National Crustal Model (Boyd and Shah, 2018), which is important for natural resource exploration and for earthquake hazard risk assessment (Shah and Boyd, 2018). In this paper, we introduce a two-step approach to gravity inversion. On the first step, we apply the 3D Cauchy-type integral representation of the gravity field to inverting gravity data for depth-to-basement model. On the second step, we use the depth-to-basement model determined on the first step as an a priori constraint for full 3D voxel-type inversion. This approach is illustrated by 3D inversion of Bouguer gravity anomaly in the Utah State.

Introduction

We have inverted the Bouguer gravity anomaly in the Utah State (Figure 1). The complete Bouguer gravity anomaly grid over the state of Utah was compiled by USGS using data from over 42,000 gravity stations. These data were extracted from the gravity data base maintained by the National Geophysical Data Center (from Department of Defense unclassified data) and augmented with data from the USGS and from several university theses and dissertations. Observed gravity relative to the IGSN-71 datum were reduced to the Bouguer anomaly using the 1967 gravity formula and a reduction density of 2.67 g/cc. Terrain corrections were calculated by USGS radially outward from each station to a distance of 167 km using a method developed by Plouff (USGS Open-file Report 77-535). The data were converted to a 1-km grid using minimum curvature techniques https://pubs.usgs.gov/of/1998/ofr-98-0761/utah_boug.html.

The inversion was conducted in two steps. On the first step, the Bouguer gravity anomaly was inverted for the depth-to-basement model using effective representation of the sediment-basement interface by surface Cauchy-type integrals, introduced by Zhdanov (1980, 1988). On the second step we ran the full rigorous inversion of the subset of Utah Bouguer gravity anomaly using the depth-to-basement model as a soft constraint in the inversion. The two-step inversion results provide one of the first 3D density distributions of the crustal model in Utah based on the Bouguer gravity anomaly data.

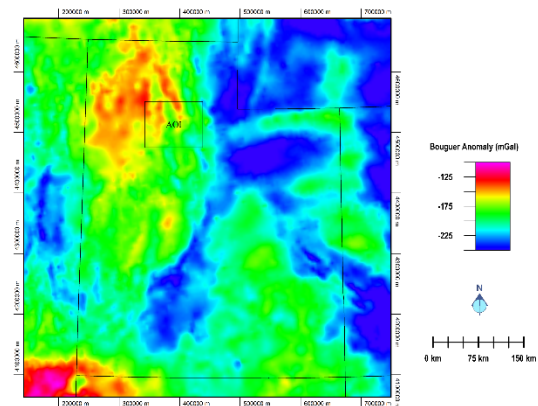


Figure 1: Utah Bouguer gravity anomaly map over the Utah State (after USGS https://pubs.usgs.gov/of/1998/ofr-98-0761/utah_boug.htm). A rectangle shown by the black line in the center of the map outlines the area of interest (AOI).

Theory

We perform a 3D inversion of the Bouguer gravity anomaly data in two steps. The first step involves the depth-to-basement inversion. The second step is 3D voxel-type inversion with the depth-to-basement used as an a priori constraint

Depth-to-basement inversion

On the first step we apply the method of 3D Cauchy-type integrals to solving both forward and inverse problems for a density contrast model (Cai and Zhdanov, 2015). This type of model is used in the inversion of the gravity data for the depth-to-basement. We assume that the surface, S , of sediment-basement interface with a density contrast, ρ_0 , is described by equation $z = h(x, y) - H_0$, and S coincides with the horizontal plane P , $z = -H_0$, at infinity.

In the framework of this approach, the gravity field, \mathbf{g} , is represented by the following formula,

$$\mathbf{g}(\mathbf{r}') = 4\pi\gamma_g\rho_0\mathbf{C}^S(\mathbf{r}', h\mathbf{d}_z), \quad (1)$$

where \mathbf{d}_z is a unit vector directed upward along vertical axis. Cauchy-type integral $\mathbf{C}^S(\mathbf{r}', h\mathbf{d}_z)$ is calculated as a surface integral of $\boldsymbol{\varphi} = h\mathbf{d}_z$ over the density contrast surface S :

$$\mathbf{C}^S(\mathbf{r}', \boldsymbol{\varphi}) = -\frac{1}{4\pi} \iint_S \left[(\mathbf{n} \cdot \boldsymbol{\varphi}) \nabla \frac{1}{|\mathbf{r}-\mathbf{r}'|} + (\mathbf{n} \times \boldsymbol{\varphi}) \times \nabla \frac{1}{|\mathbf{r}-\mathbf{r}'|} \right] ds. \quad (2)$$

The advantage of using formula (1) in forward and inverse modelling of gravity field is related to the fact that it requires

Two-step approach to 3D gravity inversion

discretization of the density contrast surface only, while the conventional algorithms are based on the volume discretization of the anomalous domain. This results in significant reduction of the memory and computing power required for 3D inversion for the depth-to-basement models.

In our inversion, the model parameter, m , is the elevations, $h = h(x, y)$, of the density contrast surface with respect to the horizontal plane P . Note that, in this case the forward operator with respect to m is nonlinear. Correspondingly, the inversion is also a nonlinear problem, and the corresponding Fréchet derivative, \mathbf{F} , is a function of model parameters which, however, can be expressed in analytical form, which simplifies the inversion algorithm.

The inversion is based on the minimization of the Tikhonov parametric functional:

$$P^{\alpha}(\mathbf{m}, d) = (\mathbf{W}_d \mathbf{A} \mathbf{m} - \mathbf{W}_d \mathbf{d})^T (\mathbf{W}_d \mathbf{A} \mathbf{m} - \mathbf{W}_d \mathbf{d}) + \alpha (\mathbf{W}_e \mathbf{W}_m \mathbf{m} - \mathbf{W}_e \mathbf{W}_m \mathbf{m}_{apr})^T (\mathbf{W}_e \mathbf{W}_m \mathbf{m} - \mathbf{W}_e \mathbf{W}_m \mathbf{m}_{apr}) \rightarrow \min \quad (8)$$

where \mathbf{W}_d is the data weighting matrix; \mathbf{m} is the vector of the model parameters, $\mathbf{m} = \mathbf{h}$, formed by the elevations, $h^{(k)} = h(x_k, y_k)$ computed on the horizontal grid (x_k, y_k) ; \mathbf{m}_{apr} is the a priori model of the density contrast model, and \mathbf{W}_m is a diagonal matrix of the model parameters weights based on integrated sensitivity:

$$\mathbf{W}_m = \mathbf{diag}(\mathbf{F}^T \mathbf{F})^{1/4} \quad (9)$$

Matrix \mathbf{W}_e is also a diagonal matrix of the minimum support stabilizer providing focusing inversion:

$$\mathbf{W}_e = \mathbf{diag}[w_e] = \mathbf{diag} \left[\frac{1}{(m_i^2 + e^2)} \right]. \quad (10)$$

The minimization of the Tikhonov parametric functional is based on the reweighted regularized conjugate gradient (RRCG) method (Zhdanov, 2002).

3D voxel-type inversion

On the second step, we apply conventional 3D inversion based on discretization of the subsurface in rectangular prisms. The regularized solution of the gravity inverse problem is based on minimization of the same Tikhonov parametric functional, (8), with the only difference that vector \mathbf{m} of the model parameters is formed by the values of the density within prismatic cells of the volume discretization grid, $\mathbf{m} = \boldsymbol{\rho}$. In addition, in the case of the voxel-type inversion, we select the a priori density model, \mathbf{m}_{apr} as the two-layers models with the density contrast surface determined on the first step of the inversion but with a relatively weak density contrast. In this case, the 3D voxel-

type inversion is guided by the results obtained by the depth-to-basement inversion, while the volume distribution of the density is adjusted in order to better fit the observed data. The details of the regularized 3D gravity inversion method can be found in Zhdanov (2015).

Case study: 3D inversion of Bouguer gravity anomaly in the Utah State

We have applied the developed approach to inversion of the Bouguer gravity anomaly, selected in the central part of the Utah State (Figure 2). The area of inversion is outlined by a black rectangle (also shown in Figure 1).

On the first step of the gravity data analysis, we inverted the data collected over this area using depth-to-basement inversion. We used the USGS depth-to-Mesozoic-basement as our initial and reference model (Shah and Boyd, 2018). The initial data misfit was poor, as we model a single interface with density contrast 0.4 g/cc; however, the inversion converged to a misfit of ~30%. Figure 3 presents an image of the density contrast surface produced by the depth-to-basement inversion. We should note that, the term “depth-to-basement” inversion should not be taken literally. In fact, we do not know if the algorithm recovers the actual surface of the crystalline basement formed by igneous or metamorphic rocks in this area. Moreover, in the western United States it is difficult to identify a specific geologic layer associate with the basement, because tectonic processes have created a very complicated geology in this area (e. g. Shah and Boyd, 2018). The surface we have recovered should be treated as a density contrast surface in the crust, which underlies the unconsolidated sediment interface. In some areas, this surface may coincide with the surface of the crystalline basement, in other areas a distinct boundary between sedimentary rock and igneous or metamorphic rock is more difficult to define.

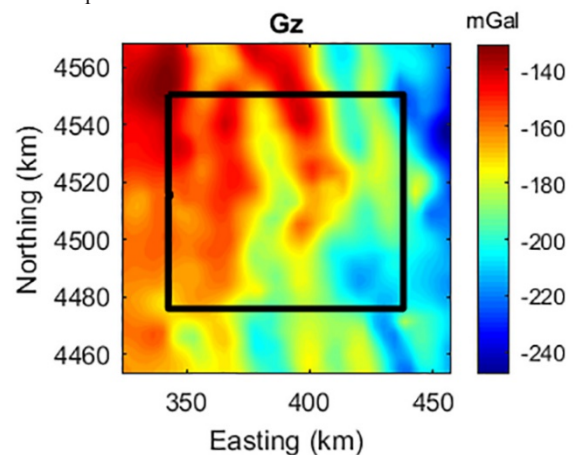


Figure 2: Bouguer gravity anomaly located in the central part of the Utah State.

Two-step approach to 3D gravity inversion

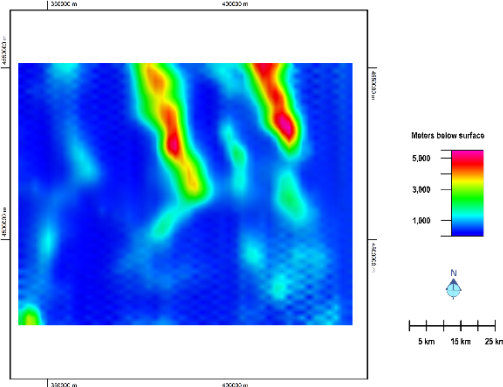


Figure 3: Map of the density contrast surface produced by the depth-to-basement inversion using the USGS model (Shah and Boyd, 2018) as our initial and reference model.

For comparison, Figure 4 presents a map of the depth-to-Mesozoic-basement produced by USGS (Shah and Boyd, 2018). In constructing this map, USGS researchers considered two quantities describing vertical dimensions of key geologic layers: (1) the thickness of unconsolidated sediments (which may also be considered as the depth to bedrock) and (2) the depth to basement. The depth was derived using various methods including seismic reflection, well data, gravity, and magnetic surveys. One can see a remarkable similarity in these two maps; however, our depth-to-basement model (Figure 3) produces the gravity anomaly which much better represents the observed data than the USGS model (Figure 4).

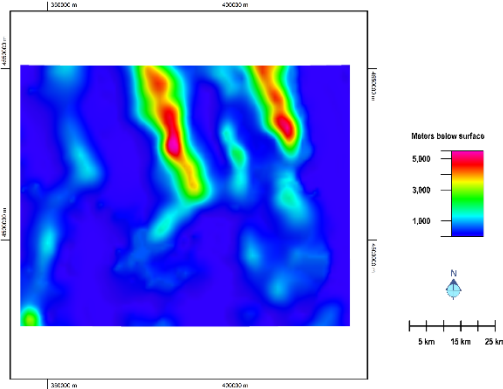


Figure 4: Map of the depth-to-Mesozoic-basement produced by USGS (Shah and Boyd, 2018).

On the second step of the gravity data analysis for the selected area, we applied conventional 3D voxel-type inversion to the filtered Bouguer gravity anomaly, shown in

Figure 5. Gravity data were filtered with a simple plane removal for inversion. The a priori model considered in the expression (8) of the parametric functional was designed using the density contrast surface shown in Figure 3 with relatively weak contrast of 0.1 g/cc. The 3D inversion domain was discretized in $99 \times 79 \times 20 = 156,420$ rectangular cells. For comparison, we have applied the inversion with and without a priori density contrast model. In both cases the iterative RRCG method was run until the misfit between the observed and predicted data reached a level of 5%.

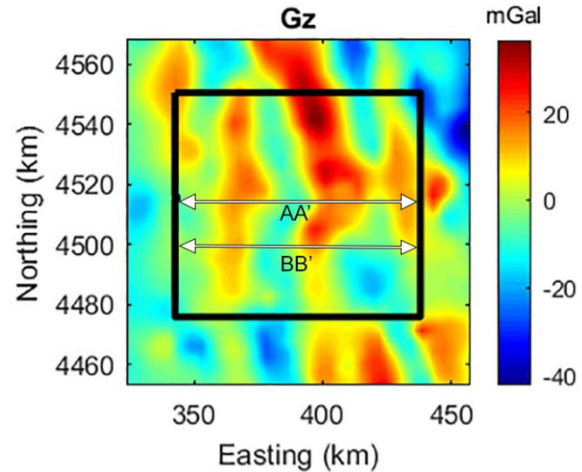


Figure 5: Filtered Bouguer gravity anomaly map. Black line shows the outline of AOI. White lines are the vertical section locations.

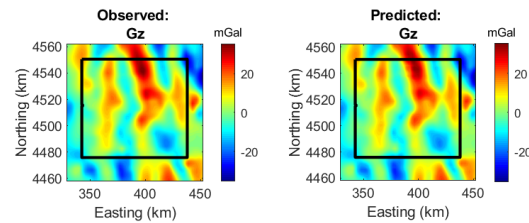


Figure 6: Comparison of the observed (left panel) and predicted (right panel) gravity data produced by 3D inversion with no a priori model.

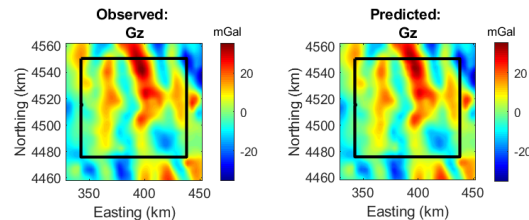


Figure 7: Comparison of the observed (left panel) and predicted (right panel) gravity data produced by 3D inversion with a priori density contrast model.

Two-step approach to 3D gravity inversion

Figures 6 and 7 show the observed and predicted gravity data obtained as the result of 3D inversion with and without a priori density contrast model, respectively. One can see that both inversions reproduce the observed data well.

We have also analysed and compared the 3D density models produced by two inversions. Figures 8 and 9 present the vertical sections along profile AA' of 3D density models produced by the inversion without a priori model and with a priori density contrast model, respectively. Similar vertical sections along profile BB' are shown in Figures 10 and 11, respectively. The outline of the a priori density contrast surface is shown by a solid line in Figures 9 and 11.

One can see that, including the a priori density contrast model in the solution of the inverse problem results in an accurate delineation of the bottom of unconsolidated sediments and the top of the basement. At the same time, our inverse density model corresponds well to the USGS model of the depth-to-Mesozoic-basement shown by the dashed line in Figures 9 and 11. This is an illustration of the ability of the guided inversion to adjust the a priori model in order to better fit the observed data. In other words, the guided inversion is not the data driven approach. The produced 3D density model of the area of interest in the central Utah provides important information about the complex geology in the area and the thickness of unconsolidated sediments.

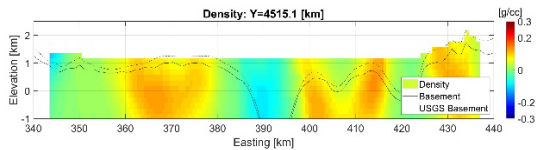


Figure 8: Vertical section along profile AA' of 3D density model produced by the inversion without a priori model.

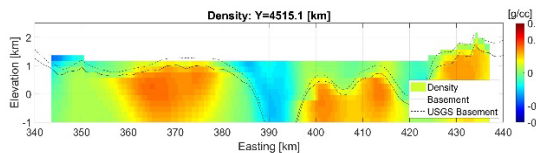


Figure 9: Vertical section along profile AA' of 3D density model produced by the inversion with a priori model density contrast model.

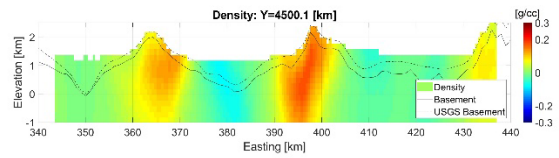


Figure 10: Vertical section along profile BB' of 3D density model produced by the inversion without a priori model.

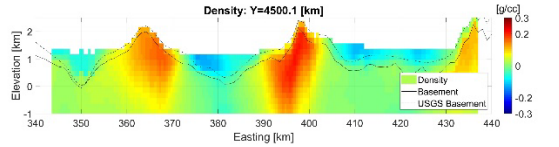


Figure 11: Vertical section along profile BB' of 3D density model produced by the inversion with a priori model density contrast model.

Conclusions

We have introduced a novel two-step approach to inversion of gravity data. This approach uses the depth-to-basement inversion on the first step to identify the surface with the strong density contrast. The produced map of the density contrast surface is used as a soft constraint (a priori model) on the second step of the voxel-based 3D inversion. We have illustrated the developed approach by inverting the Bouguer gravity anomaly data in central Utah. Comparison of the inverted density model with the depth to basement and thickness of unconsolidated sediments produced by USGS for the Western United States, demonstrates a remarkable similarity, while providing additional detailed information about the density distribution in the top layers of the earth's crust. This information could be useful for other applications such as water, mineral, and energy resource exploration. The future work will be directed at applying this approach to the entire area of the Utah State.

Acknowledgements

The authors would like to thank Consortium for Electromagnetic Modeling and Inversion (CEMI) at the University of Utah and TechnoImaging for support of this research.

REFERENCES

- Boyd, O., and A. K. Shah, 2018, National 3D geology—Building a USGS National Crustal Model—Theoretical foundation, inputs, and calibration, in L. H. Thorleifson, ed., *Geologic Mapping Forum 2018 abstracts*—Minneapolis, Minnesota Geological Survey Open File Report OFR-18-1, 13–14, March 27–29, 2018, Also available at <http://hdl.handle.net/11299/194852>.
- Cai, H., and M. S. Zhdanov, 2015, Application of Cauchy-type integrals in developing effective methods for depth-to-basement inversion of gravity and gravity gradiometry data: *Geophysics*, **80**, no. 2, G81–G94, doi: <https://doi.org/10.1190/geo2014-0332.1>.
- Shah, A. K., and O. S. Boyd, 2018, Depth to basement and thickness of unconsolidated sediments for the western United States—Initial estimates for layers of the U.S. Geological Survey National Crustal Model: U.S. Geological Survey Open-File Report 2018–1115, 13.
- Zhdanov, M. S., 1980, Use of Cauchy integral analogs in the geopotential field theory: *Annales Geophysique*, **36**, 447–458.
- Zhdanov, M. S., 1988, *Integral transforms in geophysics*: Springer-Verlag.
- Zhdanov, M. S., 2009, *Geophysical electromagnetic theory and methods*: Elsevier.
- Zhdanov, M. S., 2015, *Inverse theory and applications in geophysics*: Elsevier.